International Journal of Environmental Science and Technology (2020) 17:1113–1122
https://doi.org/10.1007/s13762-019-02547-5

ORIGINAL PAPER

Maximum discrimination index: a tool for land cover identification

A. Lencina[1] · C. Weber[2,3,4]

Received: 3 May 2019 / Revised: 30 August 2019 / Accepted: 21 September 2019 / Published online: 12 October 2019

Abstract
This work presents an adaptable index that is applied to a pair of covers to be discriminated. Its adaptability relies on the procedure to determine the numerical value of the wavelengths or bands involved: the maximization of an operator based on the geometric mean of squared differences. This index is applied to the particular case of discrimination of wheat from ryegrass in different phenological stages. The maximum discrimination index outperforms other indices such as the normalized difference vegetation index, advanced normalized vegetation index and normalized difference greenness index. Its efficacy of discrimination is characterized and compared with the normalized difference greenness index (the second with better performance). It is observed that the proposed index has a more predictable behavior and reaches a discrimination accuracy as high as 95.5%. The maximum discrimination index could be adjusted to different covers and employed as a tool for discrimination. Spectral signatures coming from any platform: field, aerial or satellite, can be handled.

Keywords Discrimination · Ryegrass · Spectral signature · Vegetation index · Wheat

Introduction

The use of spectral information to detect variations in land cover, particularly vegetation type, density and health, began several decades ago, and it is still an active area of research (Congalton 1991; Gholizadeh and Kopačková 2019; Gómez et al. 2016; Hansen and Loveland 2012; Xie et al. 2008; Xue and Su 2017). It continues today because spectra are disturbed by internal factors (plant physiological state) and/or external ones: the measurement setup, lighting, atmospheric disturbances, soil type and moisture, and the optical characteristics, spatial distribution and proportions of all the constituents of a scene (Chang et al. 2016). Then, to classify land cover features, such as the biophysical characteristics of the vegetation, many algorithms have been developed in terms of combinations of spectral bands (Buzzi et al. 2017), employing neural networks (Civco 1993), based on the inversion of radiative transfer models (Fang et al. 2003) and by multispectral approaches (Salas et al. 2016), among others. The most widely type of algorithm used is the mathematical combination of bands of visible and near-infrared reflectances, in the form of spectral indices (Xue and Su 2017).

Combinations of particular bands result in various spectral indices that have been successfully tested. They have a high sensitivity that surpasses what can be deduced by trying to interpret individual spectral bands. For this reason, more than one hundred spectral indices have been published along the last four decades (Henrich et al. 2012; Xue and Su 2017). However, there are discrepancies about the advantages and disadvantages of each index, mainly because the validations of each one do not have a universal character, but correspond to particular data groups. In this sense, it is hard to asseverate what is the most appropriate spectral index for land cover identification or characterization.

Editorial responsibility: M. Abbaspour.

✉ A. Lencina
alencina@faa.unicen.edu.ar

[1] Laboratorio de Análisis de Suelos, Facultad de Agronomía, Universidad Nacional del Centro de la Provincia de Buenos Aires, CONICET, Av. República de Italia 780, P.O. Box 47, Azul 7300, Buenos Aires, Argentina

[2] Facultad de Ciencias Agrarias y Forestales, Universidad Nacional de La Plata, Casilla de Correo 31, 1900 La Plata, Argentina

[3] Centro de Investigaciones Ópticas (CONICET-CIC-UNLP), P.O. Box 3, Cno. Centenario y 506, Gonnet 1897, Buenos Aires, Argentina

[4] Comisión de Investigaciones Científicas de la Provincia de Buenos Aires, La Plata 1900, Buenos Aires, Argentina

Different vegetation indices (VI) can highlight spectral characteristics of some vegetation type while suppressing others (Karakacan Kuzucu and Bektas Balcik 2017). Remote sensing applications for vegetation survey, such as weed–crop discrimination, have been focused on comparing leaf and canopy light reflectance properties of one vegetation type to another with the intention to identify spectral bands showing statistically significant differences among them (Fletcher and Turley 2017). Nowadays, the use of remote sensing for weed–crop discrimination is also an active field of research.

One of the best known VI is the normalized difference vegetation index (NDVI) (Rouse et al. 1974). Its success was due to its sensitivity to the presence of green vegetation, which permits the prediction of agricultural crops and precipitation in semiarid areas (Bannari et al. 1995). However, its atmospheric effects (Kaufman 1984; Fraser and Kaufman 1985) and radiometric degradation in the red and near-infrared bands (Holben et al. 1990) were appointed. As a consequence, other VI appear to deal with these issues: enhanced vegetation index (EVI) (also known as soil and atmospherically resistant vegetation index 2-SARVI2-), soil-adjusted vegetation index and modified soil-adjusted vegetation index (Henrich et al. 2012; Huete and Liu 1994; Huete et al. 1997; Huete et al. 1999; Landsat Indices 2019). However, as was previously mentioned, they were not the only indices appearing in the literature. The normalized difference greenness index (NDGI) appeared as an alternative, being sensitive to the canopy biomass and vegetation fraction or leaf area (Chamard et al. 1991; Gitelson et al. 2002; Hunt et al. 2005; Fu-min et al. 2007). Also, blue-related vegetation indexes were explored. Such is the case of the advanced normalized vegetation index (ANVI) employed to perform discrimination in vegetation (Ouyang et al. 2013; Peña-Barragán et al. 2006), among many other indices.

Based on the mathematical form of previous VI, this work introduces an index which, through a mathematical maximization procedure, allows to differentiate between pairs of spectra (or a collection of them taken in pairs). This index, baptized maximum discrimination index (MDI), is applied to the problem of differentiating annual ryegrass from wheat in different phenological stages. Its performance in relation to other VIs is comparatively studied. Besides, its efficacy and accuracy of discrimination are characterized by generating mixed spectra and compared with the best of the others VI studied.

The data recollection was performed at the Faculty of Agricultural and Forestry Sciences of the National University of La Plata in La Plata, Argentina, in the months of August and September of 2017.

This adaptable index could be applied to any pairs of land covers whose spectral signatures have been captured either in-field, by UAV or through a satellite mission.

Materials and methods

Maximum discrimination index

Based on the previous contrast index such as NDVI, NDGI and ANVI, a new contrast-based index is proposed given by

$$\mathrm{MDI}(\lambda_1, \lambda_2) = \frac{R_{\lambda 1} - R_{\lambda 2}}{R_{\lambda 1} + R_{\lambda 2}}, \tag{1}$$

where $R_{\lambda 1}$ and $R_{\lambda 2}$ are the reflectances at wavelengths (or bands) λ_1 and λ_2.

The peculiarity of this index is that λ_1 and λ_2 are not given in advance, but they are determined from the spectral signatures of the covers to be discriminated. Such determination is achieved by maximizing the geometric mean of the squared differences of the MDI between covers for all samples (e.g., phenological stages or any other feature measured), that is,

$$\mathrm{Max}\left\{\left(\prod_{k=1}^{o}\prod_{m=1}^{p}\prod_{n=1}^{q}\left(\mathrm{MDI}_{c1,k,m}(\lambda_1,\lambda_2) - \mathrm{MDI}_{c2,k,n}(\lambda_1,\lambda_2)\right)^2\right)\right\}, \tag{2}$$

where $\mathrm{Max}\{\ldots\}$ stands for the maximization operation, $c1$ and $c2$ refer to the covers to be discriminated, $k = 1 \ldots o$ list the particular situations of the covers (e.g., different combinations of phenological stages) to be considered for discrimination and $m = 1 \ldots p$ and $n = 1 \ldots q$ allude to the samples taken for each cover in each particular situation.

The choice of maximizing the geometric mean is not fanciful, but responds to a searching for an operator robust against outliers and with a similar discrimination for all particular situations. In this sense, it is well known that the geometric mean is not pushed by outliers and it is maximum if all its factors are equal.

Crop and weed sowing

To obtain the spectral signatures needed to test the MDI, wheat and annual ryegrass were grown. The plants were produced at the Faculty of Agricultural and Forestry Sciences of the National University of La Plata in La Plata, Argentina. To perform the radiometric measurements at only one date, being the different phenological stages simultaneously present, the sowing was divided into three dates: at the beginning of August; in the middle of September; and at the end of September.

Wheat cultivar Baguete® 801 was employed, whereas the Experimental Station of the National Institute of Agricultural

Technology located in Castelar, Argentina, provided the annual ryegrass (resistant to glyphosate). Pots of 10 l (23 cm diameter and 25 cm tall) with the same substrate (same optical properties) were employed to sown both species. Likewise, weed and crop were irrigated with the same frequency and intensity and phenological stage and plants health were weakly registered.

Spectral signatures

An OCEAN OPTICS USB 650 (25° FOV) spectrometer was employed to obtain wheat and ryegrass spectral signatures between 400 and 860 nm with 1 nm step. Three spectra of five samples for each phenomenological stage were acquired. The wheat (Wt) and ryegrass (Rg) phenological stages were: beginning of tillering (BT) (Z 2.1), end of tillering (ET) (Z 3.0) and reproductive stage (Rep) (Z 5.0) (Zadoks et al. 1974). To avoid soil or other environmental interferences, the sensor was placed at 5 cm to the leaf when reflectance measurements were performed. The minimization of the atmospheric disturbances with the maximum sensor sensitivity is achieved at solar noon hours of diaphanous days and that's when the measurements were made.

Signal and reference spectra were separately acquired and then post-processed to obtain the reflectance as $R_\lambda = \frac{R_{s\lambda}}{R_{i\lambda}} \times \frac{ti}{ts}$, where $R_{s\lambda}$ is the signal from the vegetation for the wavelength (λ) and $R_{i\lambda}$ is the light reference for the same λ and ti and ts are the integration times for signal and reference recordings, respectively. A Spectralon® panel was employed as reference. Care was taken to subtract darkness current in each measurement and also to adjust the integration time to exploit all the dynamic range of the sensor. Smoothing and signal-to-noise ratio maximization of the spectra were attained by averaging five contiguous spectral data and creating 5 nm bands, i.e., 400–404 nm, 405–409 nm and so on. Besides, and finally, the average of the three repetitions (for each crop in each phenological stage) was calculated by leaving the spectral signatures ready to be analyzed.

Table 1 Combinations of wheat and ryegrass in different phenological stages considered in this work

Combinations	Case k
Wh BT versus Rg BT	1
Wh ET versus Rg ET	2
Wh Rep versus Rg Rep	3
Wh BT versus Rg ET	4
Wh ET versus Rg Rep	5
Wh ET versus Rg BT	6
Wh Rep versus Rg ET	7

Data analysis

The combination of spectral signatures of the covers to be discriminated must be identified before to analyze the data. In this sense, particularizing in our case, weed–crop pairs with different phenological states were selected, according to the probability to be found in real-field situations (see Table 1). The pairs first consider weeds and crops in the same phenological states ($k = 1, 2, 3$). Secondly, combinations that are feasible to find after fallow or failed pre-emergence control of weeds were identified ($k = 4, 5$). And third, situations appearing after a poor post-emergence control were taken into account ($k = 6, 7$).

The analysis and visualization of the data were performed with Origin®, Mathematica®, Google Sheets® and Infostat®. As a first step, for overall visualization purposes all spectral signatures were averaged by classes (cultivar and phenological stage). Next, to envisage the feasibility of discrimination, the quotients crop–weed among the different combination of phenological states (Table 1) were calculated. Then, turning back to the spectral signatures without averaging, the maximization of the estimator of Eq. (2) was implemented. Once the bands were determined and to assess the performance of the MDI obtained, it was evaluated for all the combinations depicted in Table 1 and compared with the NDVI, NDGI and ANVI, according to the following expressions:

$$\mathrm{NDVI} = \frac{R_\mathrm{N} - R_\mathrm{R}}{R_\mathrm{N} + R_\mathrm{R}} \tag{3}$$

$$\mathrm{NDGI} = \frac{R_\mathrm{G} - R_\mathrm{R}}{R_\mathrm{G} + R_\mathrm{R}}, \tag{4}$$

$$\mathrm{ANVI} = \frac{R_\mathrm{N} - R_\mathrm{B}}{R_\mathrm{N} + R_\mathrm{B}}, \tag{5}$$

where R_i is the reflectance at band i = NIR, Red, Green, Blue. Also were evaluated (but not shown) the EVI (SARVI2), SAVI and MSAVI. Owing that there is not an exact prescription about the bands, as a criterion, it was selected those corresponding to the Landsat 8 mission (Landsat 8 2016). Then, Blue = 450–510 nm, Green = 530–590 nm, Red = 640–670 nm, and NIR = 845–860 nm (the latter was adjusted to the data availability from our detector). Finally, to quantify the effectiveness of discriminating crop from weed for each index, an ANOVA including a Tukey test was performed and also the geometric mean of squared differences among the average index for each combination was calculated.

MDI characterization

With the aim of characterizing the efficacy and accuracy of the MDI to detect weeds, synthetic spectra were generated.

They were obtained by linearly combining a proportion of wheat with ryegrass and ensuring that both ads to one hundred percent. Different amounts of ryegrass were evaluated ranging from zero to one hundred percent. Owing that infield, the phenological stage of wheat is assumed known, it was fixed and combined with all phenological stages of ryegrass accordingly to the situations considered in Table 1. All repetitions were taken into account to generate as many synthetic spectra as possible. For each comparison depicted in Table 1, cutoffs were defined as the weighted minimum (maximum) average value between wheat and ryegrass if VI value is lower (higher) for wheat. In some cases, two cutoffs had to be defined because wheat VI value is in between ryegrass VI value for some phenological stages. Weights were 0.9, 0.8, 0.67 and 0.5 for wheat and 0.1, 0.2, 0.33 and 0.5 for ryegrass, respectively. Then, given a proportion of ryegrass, the percentage of spectra identified as ryegrass from the total of spectra generated was evaluated. The identification was performed by calculating their MDI and comparing their values with the previously defined cutoff. A comparison with another VI was also performed. Some relevant parameters of the obtained curves were identified: (1) the amount of Rg (present in the synthetic spectra) for which 50% of spectra are identified as Rg; (2) the width of growing, the value for which the percentage of identification goes from 0 to 100%; (3) the percentage accuracy, defined as the ratio between the correctly classified spectra respect to all spectral (Wang et al. 2010; Baratloo et al. 2015). For classification, a threshold of 20% ryegrass was set (Ali et al. 2013; San Martín et al. 2016; Swanton et al. 1999). Those parameters were evaluated for all phenological stages and Rg weights of the cutoff.

Results and discussion

Figure 1 depicts average spectral signatures for crop and weed in their different phenological stages. As an overall observation, all spectra present a similar behavior: (1) a high reflectance in the NIR region appearing due to leaf structure (cellular grouping, spaces with air, chloroplasts and water content) which produces a high amount of light backscattered due to the difference between the air refractive index ($n \simeq 1$) and hydrated cellulose walls ($n \simeq 1.4$) inside the leaf structure; (2) two minima around 450–500 nm and 650–700 nm related to the chlorophyll peaks absorption; (3) a broad maximum in the green wavelengths where chlorophyll does not absorb, being this peak responsible of leaves green coloration.; (4) and finally, a secondary maximum in the blue region consequence of a valley between chlorophyll *a* and *b* absorption peaks.

The relationships between the strength and width of the two peaks in the visible range are responsible for the different nuances of greens observed in the vegetation. These subtle differences, combined with those more marked in the *NIR* region, are what we are looking for. These characteristics are what allow us to discriminate between crops and weeds. Notice that, for instance, there are several spectral signatures that cross among them. These crosses suggest changes in the spectral signature contrast, that is, changes in an index such as the proposed MDI. To enhance the visualization of these changes, the quotient between the combinations of crop and weed among their different phenological states as established in Table 1 was calculated.

Figure 2 shows the quotients of the combinations given in Table 1. In all cases, wheat was in the numerator, whereas the

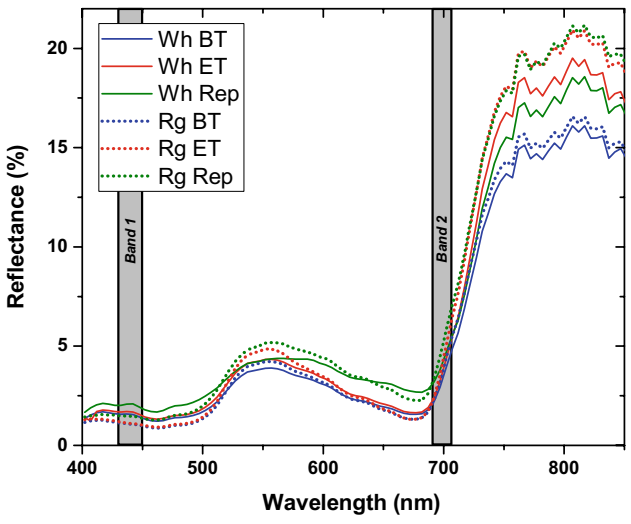

Fig. 1 Average spectral signatures of wheat (continuous lines) and ryegrass (dotted lines) at different phenological stages (blue: beginning of tillering; red: end of tillering; green: reproductive stage)

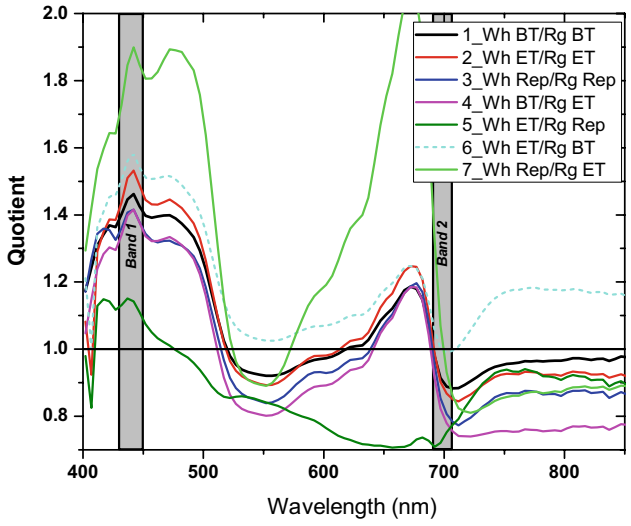

Fig. 2 Quotients among wheat (numerator) and ryegrass (denominator) average spectral signatures according to comparisons established in Table 1

ryegrass was in the denominator. In this way, if the curves in Fig. 2 are greater than one, it means that the spectral signature of wheat has a reflectance higher than ryegrass, for the phenological stages considered. On the contrary, for values lower than unity weeds have higher reflectance. From Fig. 2, it can be seen that most of the curves have well-defined regions with values above and below unity. For instance, between 400 and 500 nm all curves are higher than one, whereas above 700 nm all except one are below the unity. Several of them have a peak around 675 nm which coincides with the minimum of the spectral signatures just before the red edge. It should be noted that combination "6" has not crossed by the unity, but have marked variations with wavelength.

Given the complexity of curves depicted in Fig. 2 to identify "by hand" the proper bands which allow to discriminate all the combinations identified in Table 1, the algorithm to maximize the MDI was implemented. To take into account all the variability, it was worked with all spectra, i.e., five samples for each phenological stage. This consideration adds a total of $5 \times 5 \times 7 = 175$ factors to be considered for maximization scanning through the 92 bands and resulting in $\frac{(92 \times 92 - 92)}{2} = 4186$ elements to be compared. As a result of the maximization, two bands were identified: $\text{band}_1 = 430$–450 nm and $\text{band}_2 = 690$–705 nm (see Figs. 1, 2).

The bands maximizing the MDI differences correspond with particular features of the spectral signatures. On one hand, the band_1 is at the secondary maximum identified in the blue region which is responsible for the fine nuances in the color of the vegetation. On the other hand, the band_2 is at the beginning of the red edge. These locations present, in the whole set, the maximum contrast between crops and weeds, as can be seen in Fig. 2. Note that all combinations vary more than 40% between band_1 and band_2, reaching a 90% for the combination "7."

Figure 3 depicts the results of comparing three indexes with the proposed MDI at band_1 and band_2 found. To quantify the effectiveness in discriminating Wh from Rg, an ANOVA was performed including a Tukey test with $\alpha = 0.01$. Bars represent the average value of the index for Wh and Rg, and the same capital letter (above the bars) indicates that such average is not significantly different ($p > 0.01$). Each figure is entitled with the corresponding index. Below the title, between parentheses, the geometric mean of the squared differences (GMSD) between indices is displayed. Figure 3a shows the well-known NDVI. It is observed that for several combinations it is not possible to discriminate Rg from Wh and this is traduced in a low GMSD value. Only the Wt Rep can be differentiated from Rg Rep and Rg ET, and the NDVI of Wh BT is statistically not equal to that corresponding to Rg ET. It should also be mentioned that EVI, SAVI and MSAVI were evaluated. However,

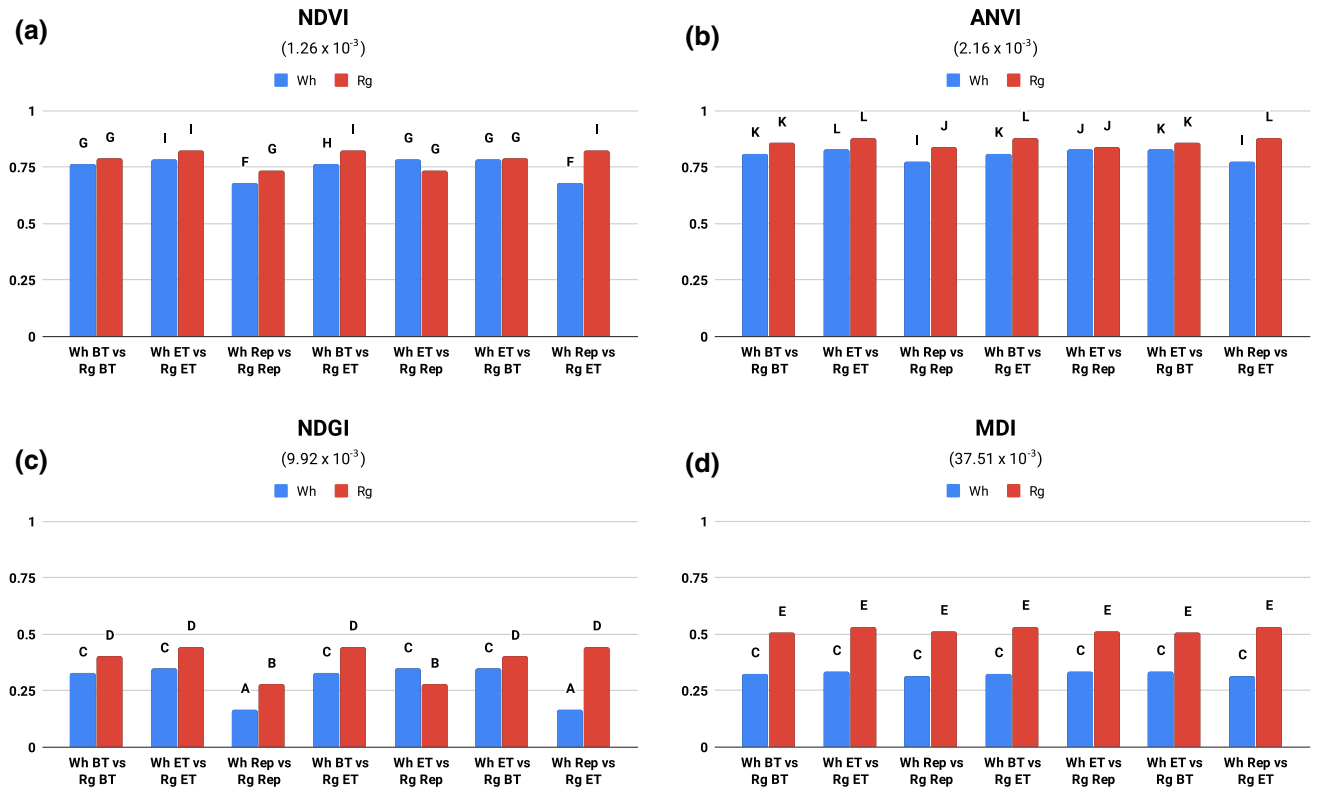

Fig. 3 Average vegetation indices (bars) calculated for the cases described in Table 1. The same capital letter (above the bars) indicates that such average is not significantly different ($p > 0.01$). **a** NDVI; **b** ANVI; **c** NDGI; **d** MDI. Value below index name corresponds to the geometric mean of squared differences

no amelioration was found when compared with the NDVI. For the ANVI, a slightly improvement in the GMSD is observed (see Fig. 3b). However, only the same three cases as in NDVI are resolved. The NDGI is presented in Fig. 3c. It is apparent that all combinations of Wh and Rg are statistically different. This fact is observed by an increase in the GMSD. All combinations means differ by only one letter with the exception of Wh Rep versus Rg Et which has a difference of three letters. Finally, in Fig. 3d the results obtained with the MDI at $band_1 = 430–450$ nm and $band_2 = 690–705$ nm are shown. From the figure, it can be observed that all combinations of Wh and Rg are clearly discriminated. All combinations differ by two letters resulting in the highest GMSD. Note that the MDI values are almost constant for each crop. Then, the MDI differences are very similar from combination to combination being this a property of the geometric mean which present its maximum when all factors are equal. In this sense, our algorithm exploits the property of the geometric mean to search for wavelengths which allow a maximum discrimination for all the combinations but tending to obtain a result equally weighted for all of them.

As a last step, and for characterizing the MDI, the efficacy of ryegrass detection is studied. For a given wheat phenological stage and a given proportion of ryegrass, all combinations

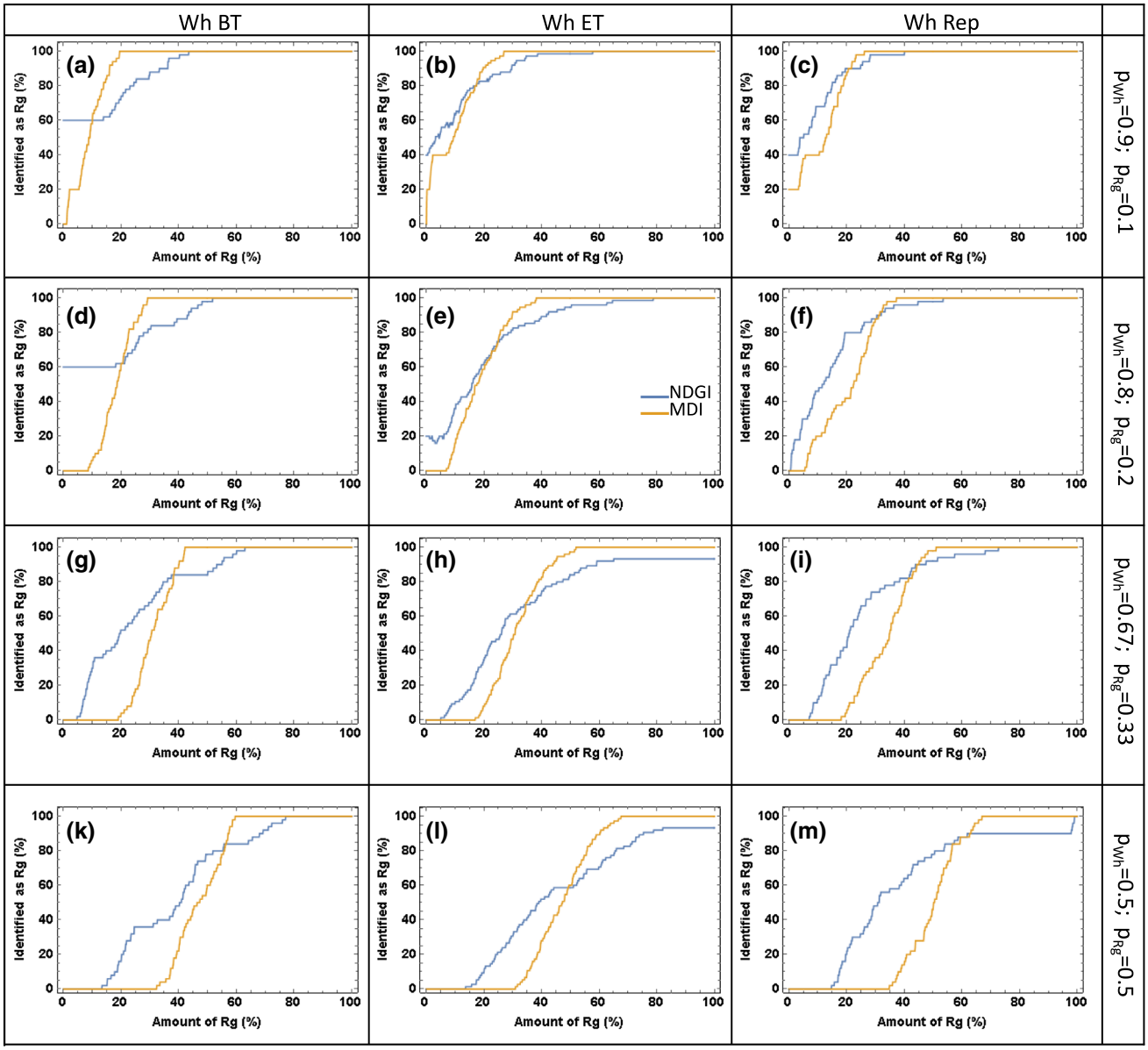

Fig. 4 Percentage of synthetic spectra (see text) identified as Ryegrass as a function of the percentage of ryegrass present in the spectra. Columns correspond with different phenological stages of wheat, whereas rows depict the weights employed to calculate the cutoffs (see text)

among repetitions with the different phenological stages of ryegrass (also with its corresponding repetitions) are evaluated. For example, consider the case of Wh BT. According to Table 1, it must be compared with Rg BT and Rg ET. Then, there are five spectra of Wh and ten of Rg giving a total of fifty spectra to be generated (the special cases are 0% of Rg with only five spectra and 100% of Rg with ten spectra). With this in mind, the analysis was performed for all phenological stages for MDI and NDGI. The results are depicted in Fig. 4 for the different weights (p_{Wh} and p_{Rg}) employed to define the cutoffs. The percentage of spectra identified as ryegrass is plotted as a function of the percentage of ryegrass present in the mixed spectra. From the figure, it is observed that NDGI starts to identify spectra as Rg before than MDI. In some cases, NDGI identify some spectra as Rg even for 0% of weed as can be seen in Fig. 4a–e. However, the percentage of identification of Rg grows slowly in comparison with the MDI. In fact, there are cases where such a percentage does not reach the 100%, still for one hundred percent of Rg in the synthetic spectra (see Fig. 4h, l) or it is achieved only for high amounts of weed such as in the case of Fig. 4e, i, m. In most cases, both curves cross at values higher than 80% of identification (see Fig. 4b, c, f, g, i, k, m). To uniformly characterize the behavior of each index, three relevant parameters were taken from the curves: the amount of Rg for which fifty percent of the spectra are identified as Rg, the width of the variation from zero to one hundred percent and the accuracy of identification. The latter is calculated based on a threshold of 20% of ryegrass in the spectra. Such results are depicted in Fig. 5.

Figure 5 resumes the relevant parameters taken from subfigures of Fig. 4. The amount of Rg as a function of the Rg weight p_{Rg} when a 50% of spectra are identified as Rg is shown in Fig. 5a. On the other hand, Fig. 5b presents the width of growing also as a function of the Rg weight p_{Rg}. Finally, in Fig. 5c, the accuracy of identification of ryegrass is presented. From Fig. 5a, it is apparent that exists a linear correspondence between abscissas and ordinates for MDI irrespective the phenological stage of the wheat. On the contrary, for the NDGI there is not a unique behavior. Regarding the width of growing shown in Fig. 5b, it can be seen that for MDI it presents a smooth linear dependence. In all cases, values are in the range of 20–30%. For NDGI, the values are higher than 45% reaching 90–95% for the cases where a 100% of identification of Rg is never attained. Moreover, the dependence with p_{Rg} is dissimilar for all phenological stages. Concerning the accuracy, it is apparent that exist an optimum weight at $p_{\mathrm{Rg}}=0.2$ where values around 95% are achieved for MDI. Such a behavior is not observed in the values of the NDGI.

The previous characterization is useful for a weed specialist to decide the better strategy to employ the MDI for crop–weed discrimination. In the same way, a similar analysis must be performed if other types of spectral signatures are studied.

The output resulting from applying the MDI to a pair of covers can be implemented in band customized cameras to be mounted in unnamed aerial vehicles.

Conclusion

This work presents an adaptable index called maximum discrimination index. It is applied to a pair of covers to be discriminated, even with particular variations such as phenological stages in vegetable coverages. The adaptability of this index resides on the way the wavelengths or bands are selected, which are not given in advance. Their numerical values are determined through the maximization of an operator based on the geometric mean of squared differences. The MDI was applied to the particular case of discrimination of wheat from ryegrass in different phenological stages. The maximization procedure gave band_1 = 430–450 nm and band_2 = 690–705 nm as the best bands to discriminate wheat from ryegrass. A comparison of MDI with other vegetation indices was performed. MDI outperformed NDVI, EVI, SAVI, MSAVI, ANVI

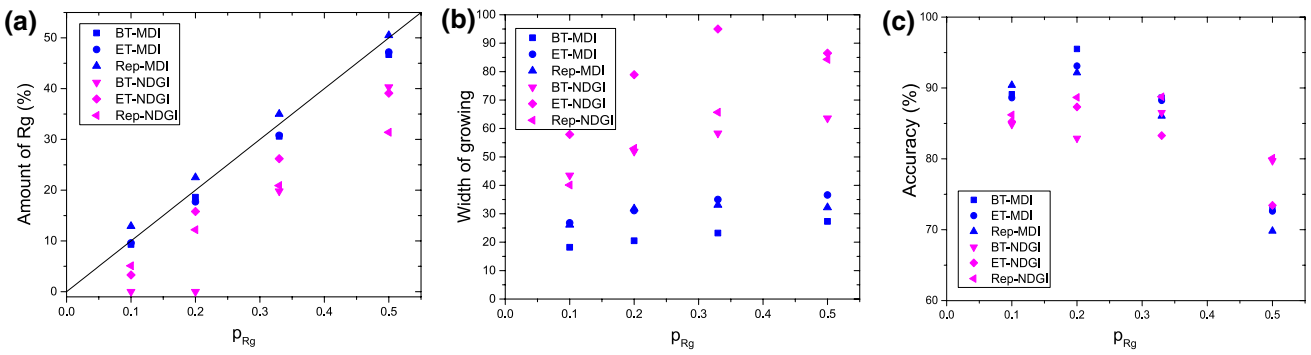

Fig. 5 Features characterizing curves in Fig. 4 as function of the weight given to the ryegrass p_{Rg} to calculate the cutoffs. **a** Amount of ryegrass present in the synthetic spectra for which fifty percent of them are identified as ryegrass. **b** Width of growing for which the percentage of spectra changes from zero to one hundred percent. **c** Accuracy of ryegrass identification assuming a threshold of 20%

and NDGI as the Tukey test confirmed. The efficacy of discrimination of the MDI was characterized and compared with the NDGI. Synthetic spectra were generated by linearly combine those of wheat and ryegrass. MDI and NDGI cutoff were calculated through weighted averages between vegetation index values of each cultivar. Four different weights and the three phenological stages were considered. The characterization focused on three features: the amount of Rg for which 50% of spectra are identified as Rg, the width of growing, i.e., the value for which the percentage of identification goes from zero to one hundred percent and the accuracy of ryegrass identification given a threshold of 20% of ryegrass present in the spectra. It was observed that the MDI has a linear correspondence with the first feature, independently of the phenological stage in which the wheat is found. In relation to the width of growing, the MDI presented lower values with a small dispersion among phenological stages. Finally, the accuracy shows that a proper selection of weights allows MDI achieve values as high as 95.5%. These results show that the MDI is an index that could be accommodated to the particular covers considered, and after an easy characterization, it can be employed as a tool for discrimination.

Acknowledgements Ch. W. thanks Universidad Nacional de La Plata and Comisión de Investigaciones Científicas de la Provincia de Buenos Aires for academically supporting this work.

Compliance with ethical standards

Data availability The data that support the findings of this study are openly available in figshare at: Navarrete et al. (2018).

References

Ali A, Streibig JC, Andreasen C (2013) Yield loss prediction models based on early estimation of weed pressure. Crop Prot 53:125–131. https://doi.org/10.1016/j.cropro.2013.06.010

Bannari A, Morin D, Bonn F, Huete AR (1995) A review of vegetation indices. Remote Sens Rev 13:95–120. https://doi.org/10.1080/02757259509532298

Baratloo A, Hosseini M, Negida A, El Ashal G (2015) Part 1: simple definition and calculation of accuracy, sensitivity and specificity. Emerg (Tehran) 3:48–49

Buzzi MA, Rueter BL, Ghermandi L (2017) Múltiples índices espectrales para predecir la variabilidad de atributos estructurales y funcionales en zonas áridas. Ecología Austral 27:055–062

Chamard P, Courel MF, Ducousso M, Guénégou MC, Le Rhun J, Levasseur JE, Loisel C, Togola M (1991) Utilisation des bandes spectrales du vert et du rouge pour une meilleure évaluation des formations végétales actives. In: Télédétection et Cartographie (ed) AUPELF-UREF, Quebec, pp 203–209

Chang L, Peng-Sen S, Shi-Rong L (2016) A review of plant spectral reflectance response to water physiological changes. Chin J Plant Ecol 40:80–91. https://doi.org/10.17521/cjpe.2015.0267

Civco DL (1993) Artificial neural networks for land-cover classification and mapping. Int J Geogr Inf Syst 7:173–186. https://doi.org/10.1080/02693799308901949

Congalton RG (1991) A review of assessing the accuracy of classifications of remotely sensed data. Remote Sens Environ 37:35–46. https://doi.org/10.1016/0034-4257(91)90048-B

Fang H, Liang S, Kuusk A (2003) Retrieving leaf area index using a genetic algorithm with a canopy radiative transfer model. Remote Sens Environ 85:257–270. https://doi.org/10.1016/S0034-4257(03)00005-1

Fletcher RS, Turley RB (2017) Employing canopy hyperspectral narrowband data and random forest algorithm to differentiate palmer amaranth from colored cotton. Am J Plant Sci 8:3258–3271. https://doi.org/10.4236/ajps.2017.812219

Fraser RS, Kaufman YJ (1985) The relative importance of scattering and absorption in remote sensing. IEEE T Geosci Remote 23:625–633. https://doi.org/10.1109/TGRS.1985.289380

Fu-min W, Jing-feng H, Yan-lin T, Xiu-zhen W (2007) New vegetation index and its application in estimating leaf area index of rice. Rice Sci 14:195–203. https://doi.org/10.1016/s1672-6308(07)60027-4

Gholizadeh A, Kopačková V (2019) Detecting vegetation stress as a soil contamination proxy: a review of optical proximal and remote sensing techniques. Int J Environ Sci Technol 16:2511–2524. https://doi.org/10.1007/s13762-019-02310-w

Gitelson AA, Kaufman YJ, Stark R, Don Rundquist (2002) Novel algorithms for remote estimation of vegetation fraction. Remote Sens Environ 80:76–87. https://doi.org/10.1016/S0034-4257(01)00289-9

Gómez C, White JC, Wulder MA (2016) Optical remotely sensed time series data for land cover classification: a review. ISPRS J Photogram Remote Sens 116:55–72. https://doi.org/10.1016/j.isprsjprs.2016.03.008

Hansen MC, Loveland TR (2012) A review of large area monitoring of land cover change using Landsat data. Remote Sens Environ 122:66–74. https://doi.org/10.1016/j.rse.2011.08.024

Henrich V, Krauss G, Götze C, Sandow C (2012) IDB-Entwicklung einer Datenbank für Fernerkundungsindizes. AK

Fernerkundung, Bochum. https://www.indexdatabase.de. Accessed 27 June 2019

Holben BN, Kaufman YJ, Kendall JD (1990) NOAA-11 AVHRR visible and near-IR inflight calibration. Int J Remote Sens 11:1511–1519. https://doi.org/10.1080/01431169008955109

Huete AR, Liu HQ (1994) An error and sensitivity analysis of the atmospheric- and soil-correcting variants of the NDVI for the MODIS-EOS. IEEE Trans Geosci Remote 32:897–905. https://doi.org/10.1109/36.298018

Huete AR, Liu HQ, Batchily K, van Leeuwen W (1997) A comparison of vegetation indices over a global set of TM images for EOS-MODIS. Remote Sens Environ 59:440–451. https://doi.org/10.1016/S0034-4257(96)00112-5

Huete AR, Didan K, Van Leeuwen W (1999) Modis vegetation index (MOD 13). Algorithm theoretical basis document. Vegetation Index and Phenology Lab, The University of Arizona. http://xurl.es/7vq1j. Accessed 1 July 2019

Hunt ER Jr, Cavigelli M, Daughtry CST, Mcmurtrey JE III, Walthall CL (2005) Evaluation of digital photography from model aircraft for remote sensing of crop biomass and nitrogen status. Precis Agric 6:359–378. https://doi.org/10.1007/s11119-005-2324-5

Karakacan Kuzucu A, Bektas Balcik F (2017) Testing the potential of vegetation indices for land use/cover classification using high resolution data. ISPRS Ann Photogram Remote Sens Spatial Inf Sci. https://doi.org/10.5194/isprs-annals-IV-4-W4-279-2017

Kaufman YJ (1984) Atmospheric effects on remote sensing of surface reflectance. SPIE Remote Sens 475:20–33. https://doi.org/10.1117/12.966238

Landsat 8, (2016) Landsat 8 (L8) Data users handbook, department of the Interior, US Geological Survey. http://xurl.es/fytzv. Accessed 3 July 2019

Landsat Indices (2019) Landsat surface reflectance-derived spectral indices. USGS Web. http://xurl.es/q6ohq. Accessed 1 July 2019

Navarrete F, Lencina A, Acciaresi H, Weber C (2018) Use of hyperspectral data to identify and discriminate wheat from a glyphosate resistant ryegrass biotype. Figshare. https://doi.org/10.6084/m9.figshare.7069835.v1

Ouyang Z, Gao Y, Xie X, Guo H, Zhang T, Zhao B (2013) Spectral discrimination of the invasive plant spartina alterniflora at multiple phenological stages in a saltmarsh wetland. PLoS One 8:e67315. https://doi.org/10.1371/journal.pone.0067315

Peña-Barragán JM, López-Granados F, Jurado-Expósito M, García-Torres L (2006) Spectral discrimination of Ridolfia segetum and sunflower as affected by phenological stage. Weed Res 46:10–21. https://doi.org/10.1111/j.1365-3180.2006.00488.x

Rouse JW, Haas RW, Schell JA, Deering DW, Harlan JC (1974) Monitoring the vernal advancement and retrogradation (Greenwave effect) of natural vegetation Type III Final Report, NASA, USA. Document ID: 19750020419. https://ntrs.nasa.gov/archive/nasa/casi.ntrs.nasa.gov/19750020419.pdf. Accessed 20 Mar 2019

Salas EAL, Boykin KG, Valdez R (2016) Multispectral and texture feature application in image-object analysis of summer vegetation in eastern Tajikistan Pamirs. Remote Sens 8:78. https://doi.org/10.3390/rs8010078

San Martín C, Andújar D, Barroso J, Fernández-Quintanilla C, Dorado J (2016) Weed decision threshold as a key factor for herbicide reductions in site-specific weed management. Weed Technol 30:888–897. https://doi.org/10.1614/wt-d-16-00039.1

Swanton CJ, Weaver S, Cowan P, Van Acker R, Deen W, Shreshta A (1999) Weed thresholds. J Crop Prod 2:9–29. https://doi.org/10.1300/9785529

Wang N, Zeng NN, Zhu W (2010) Sensitivity, specificity, accuracy, associated confidence interval and ROC analysis with practical SAS implementations. Northeast SAS user group proceedings, section of health care and life sciences, Baltimore, Maryland. https://www.lexjansen.com/nesug/nesug10/hl/hl07.pdf. Accessed 3 July 2019

Xie Y, Sha Z, Yu M (2008) Remote sensing imagery in vegetation mapping: a review. J Plant Ecol 1:9–23. https://doi.org/10.1093/jpe/rtm005

Xue J, Su B (2017) Significant remote sensing vegetation indices: a review of developments and applications. J Sens 2017:1353691. https://doi.org/10.1155/2017/1353691

Zadoks JC, Chang TT, Konzak CF (1974) A decimal code for the growth stages of cereals. Weed Res 14:415–421. https://doi.org/10.1111/j.1365-3180.1974.tb01084.x